

## Chapter 2

### Basic principles

The aim of this chapter is to introduce some basic concepts useful for the understanding of the STM experiments performed in this thesis. First, a theoretical treatment of the tunneling effect with the specific application to STM is given and the dependence of the tunneling current on the distance between tip and sample is derived. An introduction to Scanning Tunneling Spectroscopy follows. Furthermore, the Elastic Scattering Quantum Chemistry (ESQC) method which is important for calculating STM images of molecular adsorbates, is described. Finally the methods to manipulate atoms and molecules by STM are presented.

#### 2.1 Scanning Tunneling Microscopy

The STM uses the quantum mechanical tunnel effect to perform microscopy [31–35]. A metallic tip is positioned a few Angstroms above a surface and a voltage of a few Volts is applied. The potential barrier for electrons between the tip and the surface is larger than the Fermi energy of the tip or sample. Nevertheless, the electronic wave functions of the tip and the surface are exponentially decaying into the junction gap and overlap with each other. This gives rise to a tunneling current which depends exponentially on the distance between tip and surface, and it is typically in the range of nano/pico Amperes for STM measurements. To record an STM image, the tip is laterally scanned over the surface with the aid of piezoelectric elements. Using a feedback loop the tip-sample distance is adjusted in order to keep the tunneling current constant. This scanning mode is called the *constant current* mode. The vertical position ( $z$ ) of the tip is measured as a function of the lateral position on the surface ( $x,y$ ) to obtain a three dimensional mapping  $z(x,y)$  of a surface. The measured contour map  $z(x,y)$  does not simply reflect the topography of a

surface, but also contains electronic information, as will be shown in the following.

## 2.2 Scanning Tunneling Microscopy: theoretical description

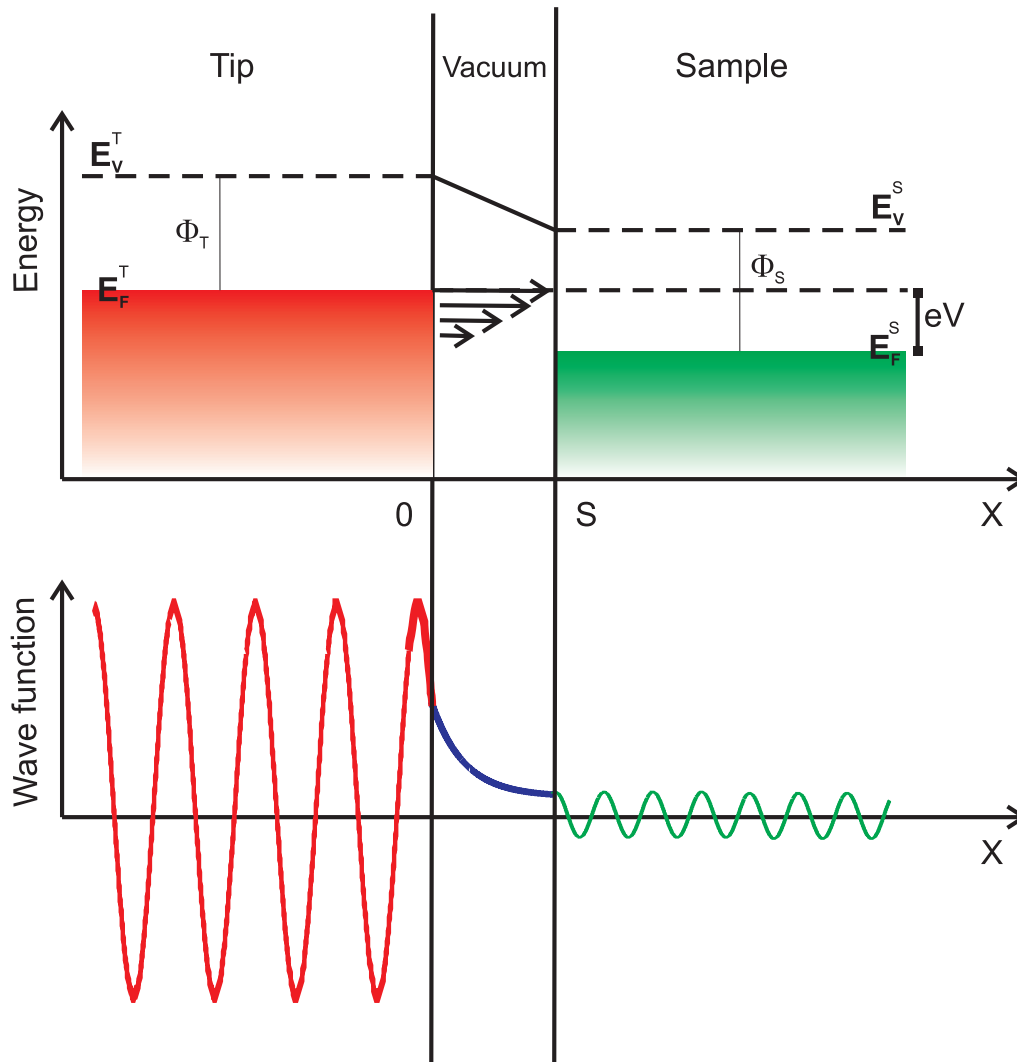


**Figure 2.1:** (Top) Schematic (in one dimension) of the energy levels of the tip and sample in a STM junction when a voltage  $V$  is applied between tip and sample and  $s$  is the barrier width.  $E_F^{T/S}$  are the Fermi energy of the tip and sample respectively, while  $E_V^{T/S}$  their vacuum levels.  $\Phi_{T/S}$  are the work function of the tip and sample respectively. (Bottom) Wave functions of an electron tunneling before, inside and after the vacuum potential barrier in the one dimensional case. For simplicity only the real part of the wave functions is shown.

In the following, I will review some theoretical concepts useful for the description of the tunneling process in STM. First of all, I will consider the simple case of one electron with energy  $E$  and mass  $m$ , tunneling through a one-dimensional rectangular potential

barrier with height  $V_0 > E$  and width  $s$ .

The Schrödinger equation which describes this system is:

$$\left[ -\frac{\hbar^2}{2m} \frac{\partial^2}{\partial x^2} + V(x) \right] \Psi(x) = E\Psi(x), \quad (2.1)$$

where  $\hbar$  is the Planck's constant divided by  $2\pi$ ,  $\Psi(x)$  is the wave function solution of the Schrödinger equation and where

$$V(x) = 0 \quad \text{for } x \notin [0, s], \quad (2.2)$$

$$V(x) = V_0 \quad \text{for } x \in [0, s]. \quad (2.3)$$

The wave functions, solutions of (2.1) have the form:

$$\Psi(x) = e^{\pm iKx}, \quad \text{for } x \notin [0, s] \quad (2.4)$$

$$\Psi(x) = e^{\pm kx}, \quad \text{for } x \in [0, s] \quad (2.5)$$

where

$$k = \sqrt{\frac{2m(V_0 - E)}{\hbar^2}}, \quad (2.6)$$

and

$$K = \sqrt{\frac{2mE}{\hbar^2}}, \quad (2.7)$$

By matching the solutions of the Schrödinger equation and their first derivatives in the three regions (before, inside and after the barrier), one obtains [36] the barrier transition coefficient  $T$ , which is the ratio of the transmitted current density and the incident current density:

$$T = \frac{1}{1 + \frac{(K^2 + k^2)^2 \sinh^2(ks)}{4K^2 k^2}}. \quad (2.8)$$

In the the limit of strongly attenuating barrier  $ks \gg 1$ ,  $T$  becomes

$$T \approx \frac{16K^2 k^2}{(K^2 + k^2)^2} e^{-2ks}. \quad (2.9)$$

Equation (2.9) shows that the dependence of the transmission coefficient on the distance  $s$  (i.e. the barrier width) is exponential. This extreme sensitivity of the tunneling transmission on the barrier width led Binnig and Rohrer [31–34] to the idea that a microscope based on the tunneling process should provide extremely high spatial resolution.

The extension of the one dimensional tunneling to the three-dimensional case has been developed by Bardeen for the generic case of a tunneling junction already in 1961, before the invention of STM [37]. He considered the two sides of the barrier (electrodes) to be very weakly coupled and treated the problem using a time-dependent perturbation theory formalism. In a similar way to the Fermi Golden rule, he calculated from the tunneling matrix element  $M_{\mu\nu}$  the probability of tunneling  $|M_{\mu\nu}|^2$  from a state  $\mu$ , described by a wave function  $\psi_\mu$ , on the left side of the barrier, to a state  $\nu$  (with wave function  $\psi_\nu$ ) on the right side of the barrier:

$$M_{\mu\nu} = -\frac{\hbar^2}{2m} \int_S d\mathbf{S} (\psi_\mu^* \vec{\nabla} \psi_\nu - \psi_\nu \vec{\nabla} \psi_\mu^*), \quad (2.10)$$

where the integral has to be evaluated over any surface  $S$ , lying entirely within the vacuum region separating the two electrodes. The transition rate from the state  $\mu$  to the state  $\nu$  is given by  $|M_{\mu\nu}|^2$ . The net current is then calculated from  $|M_{\mu\nu}|^2$  by summing over all the states on the left and right side of the barrier from which tunneling can take place and subtracting the net current in the opposite direction. Since a tunneling event is possible only from an occupied state to an empty state,  $|M_{\mu\nu}|^2$  must be multiplied by the average occupation number of one state ( $f_\mu$ ) and by the probability that the state on the right side is unoccupied, i.e. by  $[1-f_\nu]$ . This results in

$$I = \left( \frac{2\pi e}{\hbar} \right) \sum_{\mu\nu} (f(E_\mu)[1 - f(E_\nu + eV)] - f(E_\nu + eV)[1 - f(E_\mu)]) |M_{\mu\nu}|^2 \delta(E_\mu - E_\nu), \quad (2.11)$$

where  $f(E)$  is the Fermi function,  $V$  is the applied sample bias voltage and  $E_\mu$  and  $E_\nu$  are the energies of the states  $\psi_\mu, \psi_\nu$ . The delta function  $\delta$  describes the conservation of energy for the case of elastic tunneling.

Tersoff and Hamann (1983) [38,39] extended the description of Bardeen to the specific case of STM. They considered the limits of small voltage and low temperature ( $V \rightarrow 0$ ,  $T \rightarrow 0$ ), where the Fermi function has a step-shape and only energy levels near the Fermi energy  $E_F$  are important. The obtained tunneling current is:

$$I = \left( \frac{2\pi e^2}{\hbar} \right) V \sum_{ts} |M_{ts}|^2 \delta(E_s - E_F) \delta(E_t - E_F), \quad (2.12)$$

where  $E_t, E_s$  are the energy of the unperturbed wave functions of tip and sample and  $E_F$  is the Fermi energy.

Tersoff and Hamann considered a generic wave function of the sample  $\psi_s$  which decay exponentially outside the metal and propagates freely parallel to the surface plane:

$$\psi_s = \Omega_s^{-\frac{1}{2}} \sum_{\vec{G}} a_{\vec{G}} e^{-\sqrt{k^2 + |\vec{K}_{\parallel} + \vec{G}|^2} r_{\perp}} \times e^{i(\vec{K}_{\parallel} + \vec{G}) \cdot \vec{r}_{\parallel}}, \quad (2.13)$$

where  $\Omega_s$  is the sample volume,  $a_{\vec{G}}$  are coefficients,  $\vec{K}_{\parallel}$  is the surface Bloch wave vector of the state and  $\vec{G}$  is a reciprocal lattice vector.

The tip was modeled with a s-wave function  $\psi_t$ :

$$\psi_t = \Omega_t^{-\frac{1}{2}} c_t \frac{k R e^{kR}}{k |\vec{r} - \vec{r}_0|} e^{-k|\vec{r} - \vec{r}_0|}, \quad (2.14)$$

where  $\Omega_t$  is the tip volume,  $k = \sqrt{\frac{2m\Phi}{\hbar^2}}$  (above with the assumption that the work function  $\Phi$  of the tip is equal to that of the surface),  $R$  is the radius of curvature of the tip,  $\vec{r}_0$  is the center position of the tip, and  $c_t$  is a normalization parameter ( $\approx 1$ ). Within these assumptions, the matrix element  $M_{ts}$  is

$$M_{ts} = \frac{2\pi\hbar^2}{m} \Omega_t^{-\frac{1}{2}} R e^{kR} \sum_s |\psi_s(\vec{r}_0)|^2 \delta(E_s - E_F). \quad (2.15)$$

Using expressions ( 2.12) and ( 2.15) one finds

$$I = \frac{32\pi^3 e^2 V \Phi^2 R^2 \exp^{2kR}}{\hbar k^4} D_t(E_F) \cdot \sum_s |\psi_s(\vec{r}_0)|^2 \delta(E_s - E_F), \quad (2.16)$$

where  $D_t$  is the density of states per unit volume of the tip. It is now possible to define

$$\rho(\vec{r}_0, E_F) \equiv \sum_s |\psi_s(\vec{r}_0)|^2 \delta(E_s - E_F), \quad (2.17)$$

which is simply the surface local density of state (LDOS) at  $E_F$  at the position of the tip. According to this definition, at constant current and at low bias voltage the tip follows a contour of constant LDOS, provided that the s-wave function of the tip can be justified. Since in the direction normal to the surface towards the vacuum region the wave function of the sample  $\psi_s(\vec{r})$  is

$$\psi_s(\vec{r}) \propto \exp(-kr_{\perp}) \quad (2.18)$$

one finds that

$$|\psi_s(\vec{r})|^2 \propto \exp[-2k(s + R)] \quad (2.19)$$

where  $s$  denotes the distance between the sample surface and the front end of the tip. Therefore the resulting current  $I$  is given by:

$$I \propto \exp(-2ks) \quad (2.20)$$

showing once again (see equation 2.9) that the tunneling current depends exponentially on the distance between tip and sample.

### 2.3 Scanning Tunneling Spectroscopy

An important application of STM is the spatially resolved Scanning Tunneling Spectroscopy (STS) [40,41]. This technique allows one to investigate in a local way the electronic properties of a system at any given energy. Tunneling spectroscopy measurements are used in this thesis to identify molecular electronic states. In particular, in Chapter 6 a modification of the electronic structure of an azobenzene derivative upon isomerization has been identified by STS measurements and represents a fingerprint of two valence isomers.

For zero bias voltage applied between tip and sample (see Fig. 2.2(a)) the Fermi levels of the tip and sample are aligned at equilibrium. When a voltage  $V_s$  is applied to the sample, the energy levels of the sample are rigidly shifted by an amount  $|eV_s|$ . For positive applied voltages (Fig. 2.2(b)), the electrons tunnel from occupied states of the tip to unoccupied states of the sample, while at negative bias (Fig. 2.2(b)), the electrons tunnel from occupied states of the sample to unoccupied states of the tip. Hence, by varying the applied voltage one can select the electronic states involved in the tunneling process. At a given energy  $eV$ , the tunneling current is given by:

$$I \propto \int_0^{eV} D_t(\pm E \mp eV) D_s(E) dE, \quad (2.21)$$

where  $D_t$  and  $D_s$  are the tip and sample densities of states respectively. Under the assumption that the density of states of the tip has no variation within the energy range of measurements (i.e.  $D_t = \text{const}$ ), it follows that

$$\frac{dI}{dV} \propto D_s(eV), \quad (2.22)$$

i.e. , the first derivative of the tunneling current reflects, to a first approximation, the electronic density of states of the sample at the energy  $E=eV$ . The value of  $dI/dV$  can be

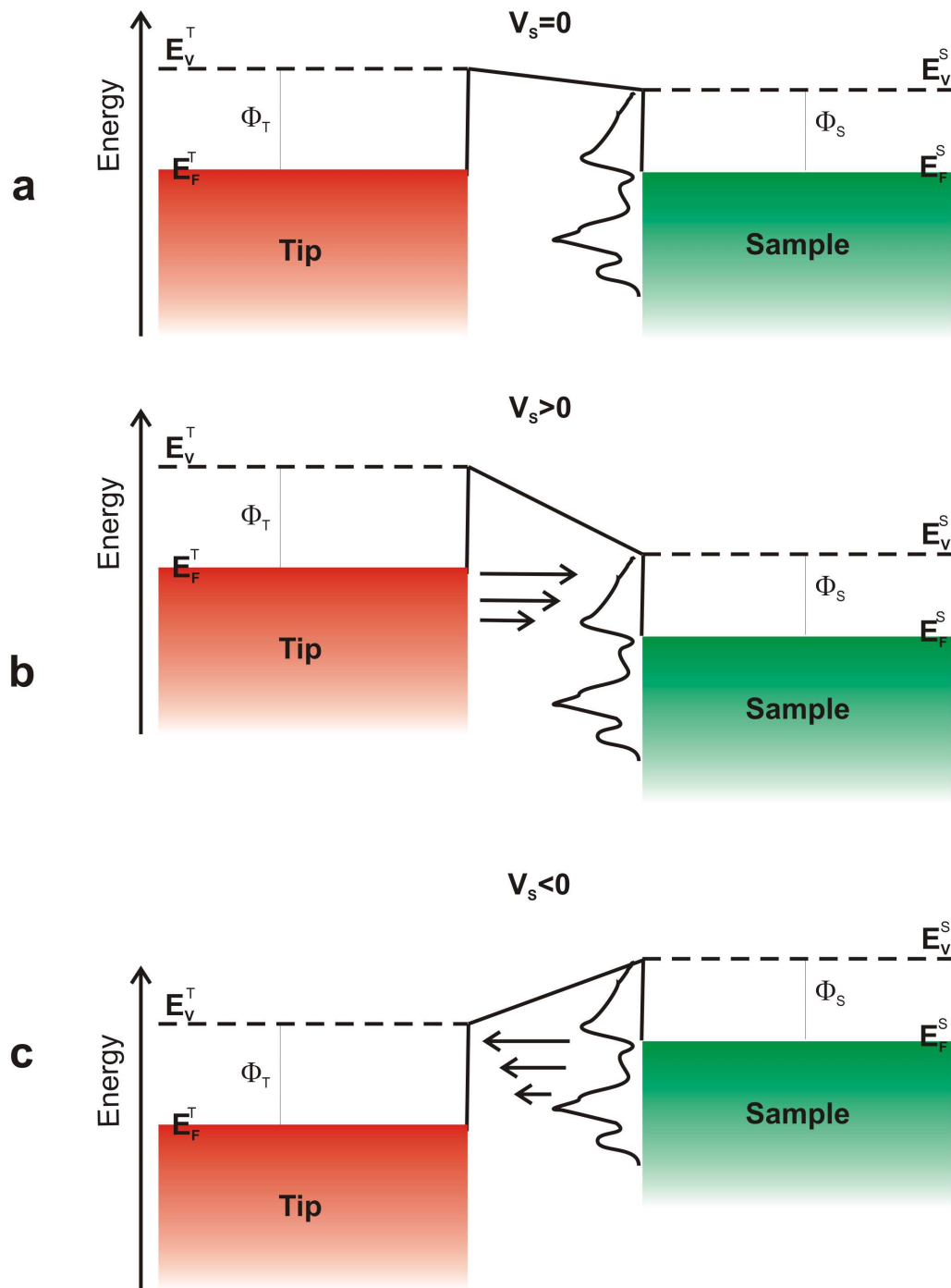


**Figure 2.2:** Energy level diagrams for tip and sample under the approximation of constant local density of states of the tip.  $E_V^{T/S}$  are the vacuum levels,  $E_F^{T/S}$  the Fermi energies,  $\Phi_{T/S}$  the work functions of tip/sample respectively. (a) When no bias voltage is applied ( $V_s=0$ ), the tip and the sample are in equilibrium. (b) When a positive voltage is applied to the sample the electrons tunnel from the tip to the sample. (c) When a negative voltage is applied to the sample the electrons tunnel from the sample to the tip.

directly obtained experimentally: the STM tip is positioned at the desired position (x,y) of the sample. The bias voltage applied between the tip and the sample is varied in the desired energy range. A high-frequency sinusoidal modulation voltage is superimposed on the constant d.c. bias voltage. The resulting tunneling current modulation, which is in phase with the applied voltage modulation, is recorded with a lock-in amplifier. Its signal at the modulation frequency corresponds to  $dI/dV$ .

## 2.4 Elastic Scattering Quantum Chemistry

For the interpretation of STM images of molecules, on surfaces one usually needs theoretical modeling. In fact, the information which one can obtain about molecular adsorption from STM images is limited, in particular in the case of large complex molecules. In this thesis experimentally measured STM images of Lander molecules on a copper surface will be compared to calculations with Electron-Scattering Quantum-Chemistry (ESQC) method in Chapter 4, allowing the determination of the exact molecular conformations.

Several theoretical approaches can be found in the literature for the calculations of molecules on metallic surfaces. An STM image of an adsorbed molecule was first approximated [42,43] by a contour map of constant probability density of the HOMO (highest occupied molecular orbital) or LUMO (lowest unoccupied molecular orbital) of the molecule, as in the case of a clean surface where an STM image is the contour map of constant Fermi-level LDOS of the substrate in the absence of the tip (see section 2.2). However, the comparison of the free molecule electron-density map with experimental data of the molecule adsorbed on the metal surface is problematic since molecular orbitals can be shifted and modified by the presence of the surface.

Other approaches use the Bardeen theory for the three dimensional tunneling problem and the calculations of Tersoff and Hamann based on an s-wave model of the tip [44]. These approaches however have some drawbacks since a realistic STM tip is a cluster of atoms, which cannot be represented by a s-wave function. Moreover, the Bardeens approach assumes weak coupling between the tip and the substrate and it is valid only for large tip-sample distances when the adsorbate is not deformed by the tip.

To simulate the image of a molecular adsorbate in a better way, Sautet and Joachim [45] proposed the Electron-Scattering Quantum-Chemistry (ESQC) method, having two particular advantages. First, its validity is not restricted to large tip heights. It can there-



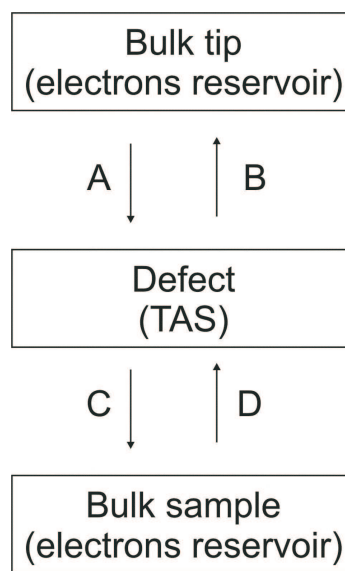


**Figure 2.3:** Schematic representation for the elastic scattering quantum chemistry (ESQC) method of the junction "tip apex-adsorbate-substrate" (TAS) and the connection with the electron reservoir of the tip and sample bulks. The incoming (A,D) and outgoing (B,C) waves amplitudes are indicated.

fore be used at tip-to-substrate distances occurring in real STM experiments. Second, ESQC takes into account the full geometry of the tip-adsorbate-substrate, being able to model any lateral interactions which may arise between the tip and the adsorbate. The Elastic-Scattering Quantum-Chemistry method treats the tunneling of an electron through an STM gap as a scattering event [45–47], as shown in Fig. 2.3: the "tip apex-adsorbate-substrate" (TAS) represents a defect which breaks the translational invariance of the tip bulk and the substrate bulk. This defect scatters an incident electron. The TAS is connected to an electron reservoir (tip and sample bulk). The junction is described using a matrix representation and it is modeled by the symmetric system  $\dots\text{XXX}\text{Y}\text{XXX}\dots$ , where X symbolizes a periodically repeated cell and Y symbolizes the defect. The total wave function is represented, in the tight-binding approximation, as a linear combination of the atomic orbitals taking into account the complete chemical description of the tip, of the adsorbate, and of the substrate. To simplify the calculation of the tunneling current, the lateral dimensions of the TAS and of the surface are reduced to those of the tip apex with adequate boundary conditions. The method ignores both electron-electron and electron-phonon interactions which may occur during the scattering, and assumes that the scattering is elastic. This assumption is fulfilled for a mean free path of the electron larger

than the size of the defect and therefore the model is valid for the typical tip-to-substrate distances encountered in STM.

The tunneling current through the TAS is calculated from the scattering matrix  $S(E, x, y, z)$ , which relates the amplitudes of the outgoing waves to those of the incoming waves on the defect. If  $A$  and  $D$  (as shown in Fig. 2.3) are the amplitudes of plane waves traveling through the defect (TAS), the scattering matrix  $S(E, x, y, z)$  is defined by:

$$\begin{pmatrix} C \\ B \end{pmatrix} = S(E) \begin{pmatrix} A \\ D \end{pmatrix}.$$

In order to calculate  $S(E, x, y, z)$  one uses the transfer matrix  $T(E, x, y, z)$  [45], which describes the amplitudes of the waves propagating from the left of the TAS to the right and is defined by:

$$\begin{pmatrix} C \\ D \end{pmatrix} = T(E) \begin{pmatrix} A \\ B \end{pmatrix}.$$

Finally, the transmission coefficient  $t(E, x, y, z)$  of an electron at a given energy  $E$  and a given position  $(x, y, z)$  of the tip apex on the surface

$$t = \frac{|C|^2}{|A|^2},$$

can be calculated from the scattering matrix  $S(E, x, y, z)$  [45]. At low bias voltage  $V$ , the conductance ( $G$ ) of the junction is given by the generalized Landauer formula [48]:

$$G = \frac{I}{V} = \frac{e^2}{\pi\hbar} t(E_F), \quad (2.23)$$

where  $t(E_F)$  is the transmission coefficient for an electron at the Fermi energy  $E_F$  with no applied bias voltage. From this equation the electronic current  $I(x, y, z)$  passing through the TAS is obtained as

$$I(x, y, z) = G(x, y, z)V, \quad (2.24)$$

From the  $I(x, y, z)$  map, a constant height or a constant current STM image can be calculated.

To calculate STM images of molecular adsorbates using this method, the exact conformation of the molecule on the surface is needed. This is normally obtained by molecular mechanics (MM) calculations. MM is a method based on Newtonian mechanics in which the molecular geometry is optimized minimizing the energy of the system which is described as a function of the atomic coordinates.

## 2.5 Manipulation of atoms and molecules by STM

The tip of an STM can be used to manipulate single atom or molecule adsorbed on a surface [12]. Under the general term "manipulation", many different kinds of modifications of an adsorbate are grouped [15–17]. Manipulation by STM is, for example, the controlled positioning of an atom/molecule on a surface [12–14, 18, 27, 49–55], the induction of the conformational change inside a single molecule [20, 56, 57], induction of motion [22–25] or even the modification of the chemistry of a single molecule [29, 30, 58–60]. In this sense, the STM constitutes a very powerful tool, being able to construct nanostructures, control properties of single molecules with diverse functionalities, induce chemistry at the molecular level, and simultaneously image the manipulation results with atomic resolution.

To induce atomic and molecular manipulation with a STM, one must control three parameters: tip-sample distance, bias voltage and tunneling current (actually determined by the other two). By tuning these parameters, different interactions can be used for the manipulation: atomic forces, tunneling electrons or electric field forces.

In this thesis, the technique of manipulation of adsorbed molecules has played a crucial role. On the one hand, it has allowed to study the deformation of a molecule during its lateral movement, as described in Chapter 4. Furthermore, it has given information on the molecule-substrate interaction as well as about tip-molecule interaction. Moreover, in Chapter 6, manipulation has been used to induce the reversible *cis-trans* isomerization of an azobenzene derivative on a surface in a controlled way. Due to the particular importance of manipulation in this thesis, I will describe the different mechanisms of manipulation by STM detailed in the following.

### 2.5.1 Atomic forces

If the tip is positioned very close to the surface atomic forces are established, even in the absence of an applied bias voltage. These forces contain both Van der Waals and electrostatic contributions. By adjusting the position of the tip, one can tune the magnitude and the direction of the force between tip and adsorbate and use it to move the adsorbate to a new position on the sample [12, 14]. The manipulation procedure is shown in Fig. 2.4: (a) First the tip is positioned above the adsorbate and the tip height is decreased, thereby

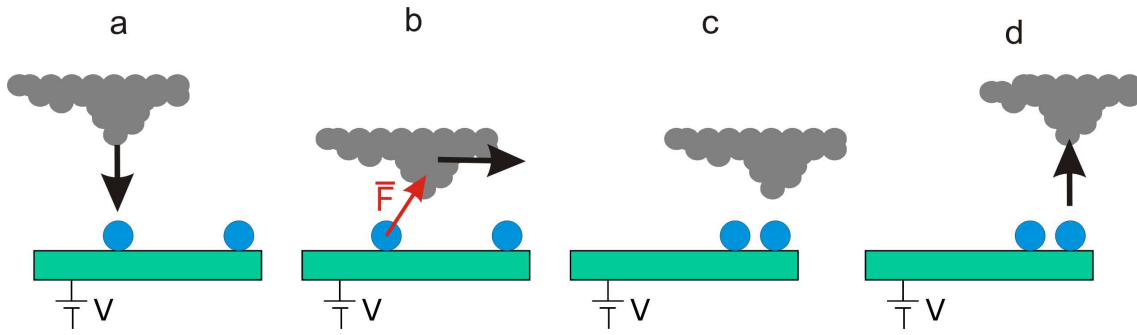


**Figure 2.4:** Schematic illustration of the lateral manipulation process. (a) The tip is positioned on an adsorbate and the tip height is reduced so that chemical forces are formed.  $\vec{F}$  is in the schematic the force between tip and adsorbate. The tip is then moved laterally (b) to the desired position of the substrate (c). In (d) the tip height is retracted so that the tip-adsorbate interaction is negligible.

increasing the tunneling current. (b) Then the tip is moved laterally until it reaches the desired position of the substrate (c). During this motion the adsorbate is dragged by the tip. Finally (d) the tunneling current is again reduced so that the tip is retracted and does not exert any interaction on the adsorbate. During the manipulation, the adsorbate never loses contact with the surface. Therefore, this kind of manipulation is called *lateral manipulation*. In contrast, in the *vertical manipulation* mode, the adsorbate is vertically captured by the tip and then released in a new position on the sample [18]. The lateral manipulation method has been used by Eigler and Schweizer [12] in the very first manipulation experiment to slide Xe atoms on a Ni(110) surface in order to assemble a nanostructure forming the logo of IBM. In our group manipulation with atomic forces have been extended to small [14, 53] and large molecules [54, 55].

During the lateral manipulation, one can record the tip height (current) signal while the STM tip is moved in constant current (or height) mode. By studying the signal recorded during the lateral movement of the tip one can extract the adsorbate motion on the surface and the kind of tip-adsorbate interaction that is involved during the manipulation [52]. Three different manipulation types can be recognized: *pulling*, *pushing* and *sliding* [52], that depends on the tip-adsorbate force. They are schematized in Fig. 2.5 for the case of constant current mode. In the *pulling* mode (Fig. 2.5(a)) the adsorbate is manipulated via an attractive tip-adsorbate interaction. During the manipulation the adsorbate is behind the tip apex and it follows the tip discontinuously by hopping from one adsorption site to

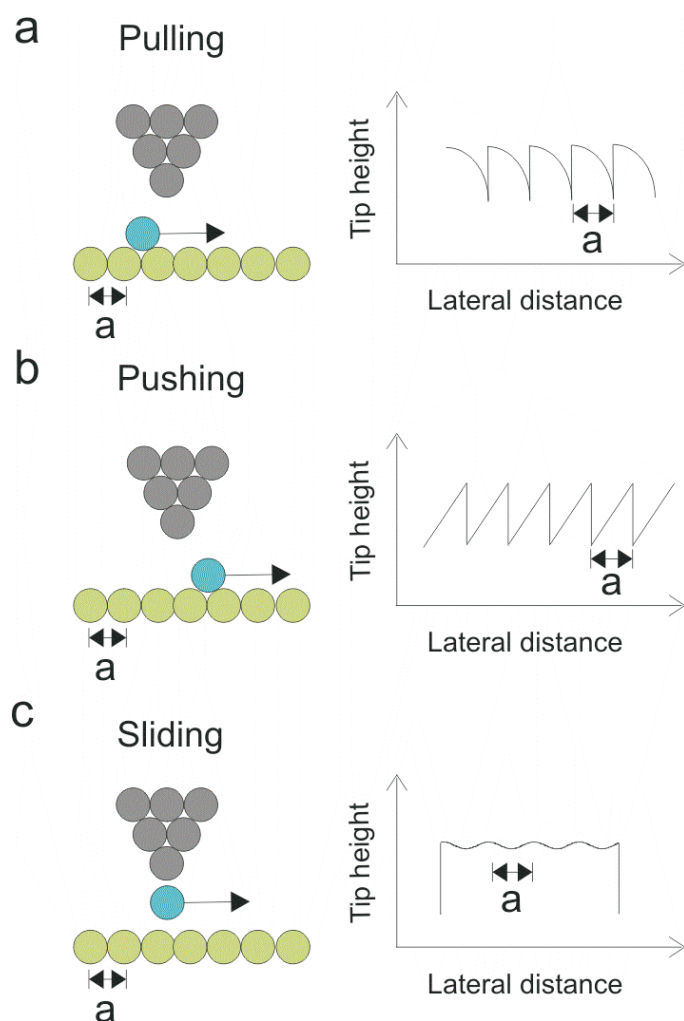


**Figure 2.5:** Schematic of the different modes of lateral manipulation in constant current and their respective signals. (a) Pulling mode, (b) pushing mode and (c) sliding mode. In the schematics  $a_0$  indicates the lattice constant.

the next. When the adsorbate jumps towards the tip, the tip height signal suddenly increases in order to keep the tunneling current constant. Then, the tip follows the LDOS of the adsorbate on the surface (one observes a decrease of the manipulation signal with a finite slope) until the molecule jumps again to an adsorption position underneath the tip (and the tip height increases again). The periodicity of the signal corresponds to the distance between adsorption positions of the adsorbate during the manipulation (in Fig. 2.5 it corresponds to the lattice constant). During a *pushing* process (Fig. 2.5(b)), the adsorbate is in front of the tip and is pushed by the advancement of the tip apex due to repulsive forces. The tip height signal increases (with a finite slope) as the tip approaches the adsorbate, then suddenly drops when the adsorbate jumps away. By reducing the tip-adsorbate distance with respect to the pulling case, an adsorbate can be manipulated by attractive forces in a continuous way (*sliding* mode in Fig. 2.5(b)). During the *sliding* mode the tip-adsorbate interaction is so strong that the adsorbate remains bound under the tip apex

during the manipulation path. In this case, the manipulation signal corresponds to the surface corrugation scanned by the tip-adsorbate system.

In another important manipulation experiment it has been shown that the signal, recorded during the manipulation of a large molecule, contains detailed information about the deformations inside the molecule [55]. Low temperatures are not always necessary for lateral positioning of the adsorbate by STM [50], but they are needed to study of the manipulation signal. A special kind of vertical manipulation has been used to mechanically induce conformational changes inside a specially designed porphyrin-based molecule [20] thus realizing the principle of a conformational molecular switch.

### 2.5.2 Tunneling electrons

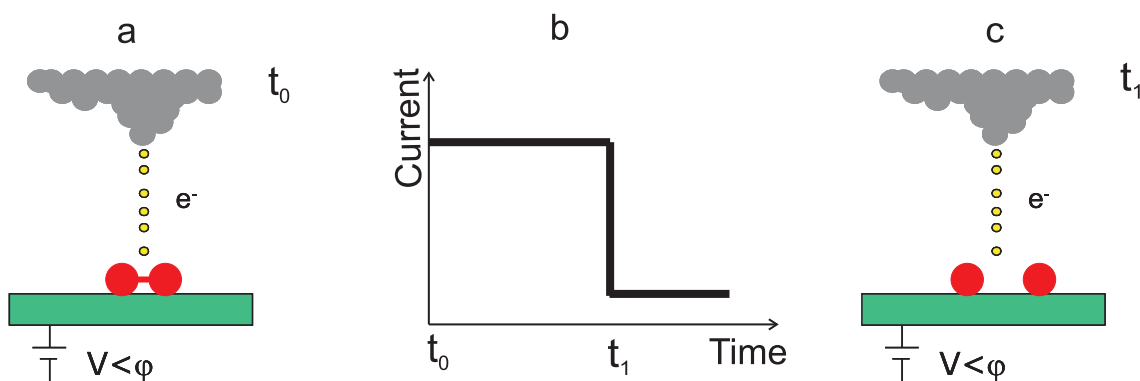


**Figure 2.6:** Manipulation scheme with tunneling electrons in the case of molecular dissociation. (a) The tip is positioned directly above an adsorbed molecule. At time  $t_0$  a voltage pulse is applied. The value of the applied voltage  $V$  is smaller than the work function  $\varphi$  of the tip or sample. (b) During the application of the pulse, the tunneling current is measured as a function of the time. (c) At the time  $t_1$ , when the manipulation takes place (the molecule has dissociated), the current signal decreases abruptly.

Manipulations can be induced using the electrons of the STM junction. Tunneling electrons are localized to atomic dimensions ( $< 1 \text{ \AA}$  around the position of the tip). Due to this high spatial resolution, modifications of selected bonds inside a single molecule are possible. Tunneling electrons were used to reversibly transfer a Xe atom between the STM tip and a Ni(110) surface realizing an atomic switch [18], or to dissociate and desorb  $O_2$  molecules on Pt(111) [22], or to induce the rotation of a biphenyl molecule on Si(100) [23]. Electrons or holes are injected into the system by applying voltage pulses. During the application of the pulse the current signal is recorded versus time (see Fig. 2.6).

As schematically shown in Fig. 2.6(b), an abrupt change in the current is detected if the manipulation is successful.

By varying the pulse voltage one controls the energy of the tunneling electrons, while the number of electrons inserted in the system are changed by the tip-sample distance. By tuning these parameters it is possible to control the reaction rate and pathways [17].

Different mechanisms may drive the manipulation with tunneling electrons. For example, in the case of Xe atom transfer on the tip [18] and O<sub>2</sub> dissociation on Pt(111) [61], it has been argued that the vibrational modes of the atom surface system or the molecule are excited by inelastic tunneling of electrons. A tunneling electron inelastically scattered from the adsorbate, transfers energy to the vibrational modes of the adsorbate. In order to overcome the potential energy barrier to activate the switch or to dissociate O<sub>2</sub> molecules, one or multiple vibrational excitations in the ground electronic state are needed. Therefore one or multiple inelastic scattering processes are required. In contrast, the rotation of biphenyl molecule on Si(100) has been associated with electronic excitation of molecular resonances [23].

### 2.5.3 Electric field

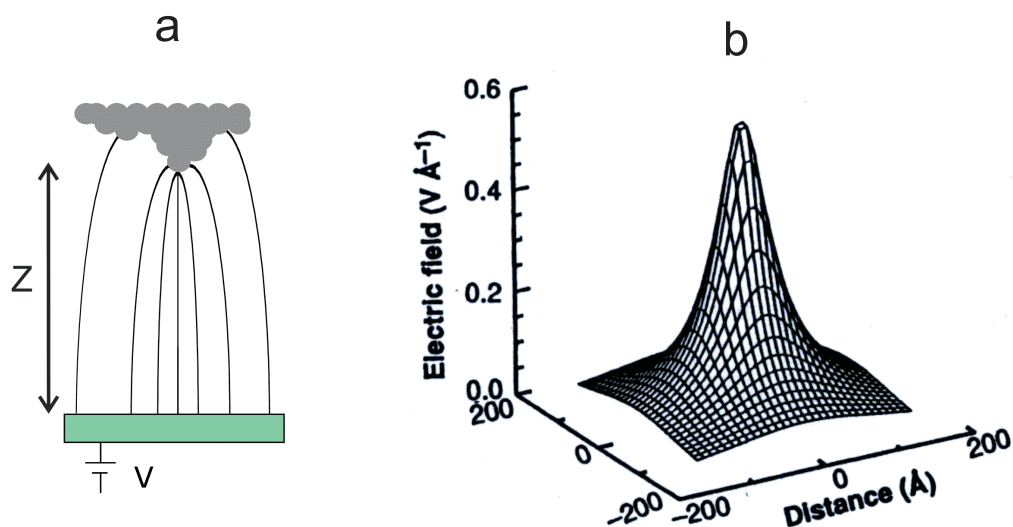


**Figure 2.7:** (a) Schematic of the electric field in the STM junction.  $V$  is the voltage applied between tip and sample, while  $z$  is the tip apex-sample separation. (b) Calculation from Ref. [13] of the electric field spatial dependence considering the STM tip as a sphere with radius 100  $\text{\AA}$  positioned 5  $\text{\AA}$  above a planar metallic surface. The potential difference is 3 V.

If a bias voltage is applied between the STM tip and the surface, a static electric field is created, which can be used to manipulate atoms or molecules [28, 62, 63]. The strength of such an electric field is very large, due to the close proximity of the tip to the surface (Fig. 2.7). Its value (typically about  $\sim 10^8$  V/cm) can be compared with the fields experienced by electrons in atoms or molecules<sup>1</sup>. Unfortunately, the exact shape of the field is not known because it depends on the atomic structure of the tip, which is never exactly known. The electric field is concentrated, in an inhomogeneous way in the vicinity of the tip-apex, but its extension can reach several hundred Angstroms. Fig. 2.7(b) shows a calculation performed by J.A. Stroscio and D. M. Eigler [13] of the electric field in the STM junction. The tip is modeled as a sphere with radius 100 Å positioned 5 Å above a planar metallic surface with a potential difference of 3 V.

An atom or molecule in a homogeneous electric field  $\vec{E}$ , is exposed to an effective potential  $U(\vec{r})$  defined as

$$U(\vec{r}) = U_0(\vec{r}) - \vec{\mu} \cdot \vec{E}(\vec{r}) - \frac{1}{2} \vec{\alpha} \vec{E}(\vec{r}) \cdot \vec{E}(\vec{r}) \quad (2.25)$$

where  $U_0$  is the field free potential energy of the adsorbate,  $\vec{\mu}$  is the static dipole moment,  $\vec{\alpha} \vec{E}$  is the induced dipole moment, and  $\vec{\alpha}$  is the polarizability tensor. The interaction of an adsorbate with such a strong electric field in the STM junction has been first used to position Cs atoms on a semiconductor surface [27]. In this case the interaction between the dipole moment of a Cs atom and the electric field induced a potential energy gradient along the surface, which allowed atomic lateral positioning. Notice that Eq. 2.25 shows that the component of dipole moment depends on the sample voltage polarity, while the polarizability term does not. Notice furthermore that the polarizability term is the basis of "optical tweezers" in which a molecule or larger object is manipulated by the electric field of a laser beam [64].

It is important to note that this kind of manipulation is operative even in the limit of zero tunneling current.

Another kind of manipulation by applying an electric field is possible when the voltage applied overcomes the value of the work function of the tip or surface and electrons are field emitted [65].

---

<sup>1</sup>The atomic unit of the electric field is  $5 \times 10^9$  V/cm.



Notice that the strong electric field created by a sharp tip when a positive voltage is applied to it is used in the Field Ion Microscopy (FIM), introduced in 1951 by E. Mueller [66], which was the first experimental method capable of atomic resolution.

